

Also, some 20-100 nm ruthenium particles were observed, while the fresh catalyst analysis had not shown any visible ruthenium particles.

5.2.1.1.2 Tests at H₂:CO Feed Ratio = 2.9, 208°C at Inlet and 35 atm

In an attempt to suppress formation of the volatile ruthenium carbonyl species and thereby prevent ruthenium metal agglomeration, another highly dispersed ruthenium Catalyst 4966-72 was tested in Run 18 at a lower CO partial pressure (Tables 5-20 and 5-21 and Figures 5-107 through 5-113). The CO pressure was lowered relative to that in Run 16 by increasing the H₂:CO feed ratio from 0.9 to 2.9. Other conditions were 208°C at the inlet, 35 atm and 70 GHSV. In this run the pressure test at 208°C lasted unusually long (4 days) due to leaks in the reactor system.

The initial CO conversion was 35%, which is higher than that observed in Run 16, probably because of the higher H₂ partial pressure (Figure 5-107). The CO conversion decreased during the run, apparently because of the rapid decrease of catalyst's water gas shift activity (Figure 5-108). The CO+H₂ conversion, on the other hand, remained steady at about 15% level. At 60 hours on stream there was a plant upset, and the flow in and out of the reactor was stopped for about 10 hours. Interruption of the flow caused high conversion of the feed gas inside the reactor. After the flow was reinstated the catalytic performance gradually reached the level it had before the upset. It is important to note that during the 10-hour-period in which the flow was interrupted the selectivities to C₂-C₄ hydrocarbons increased and the olefin to paraffin ratios decreased (Figures 5-109 and 5-110). With ruthenium catalysts, C₂-C₄ hydrocarbons, particularly the olefins, are typically made with selectivities below the Anderson-Schulz-Flory prediction. These results, then, suggest that under long contact time, no-flow conditions reaction pathways which result in selective disappearance of C₂-C₄ hydrocarbons are not favored, possibly because of the saturation of the olefins.

Table 5-21. Hydrocarbon Distributions in Run 18

C1	12.5690	C51	0.4886	C101	0.1404	C151	0.0313	C201	0.0083
C2	1.4168	C52	0.4690	C102	0.1361	C152	0.0305	C202	0.0063
C3	5.0750	C53	0.4500	C103	0.1319	C153	0.0297	C203	0.0062
C4	4.9954	C54	0.4324	C104	0.1278	C154	0.0280	C204	0.0061
C5	2.9912	C55	0.4170	C105	0.1238	C155	0.0283	C205	0.0060
C6	1.5732	C56	0.3654	C106	0.1199	C156	0.0276	C206	0.0059
C7	2.6214	C57	0.3561	C107	0.1150	C157	0.0270	C207	0.0058
C8	4.2662	C58	0.3493	C108	0.1115	C158	0.0264	C208	0.0057
C9	4.7566	C59	0.3444	C109	0.1081	C159	0.0258	C209	0.0056
C10	3.9928	C60	0.3406	C110	0.1048	C160	0.0252	C210	0.0055
C11	3.1943	C61	0.3375	C111	0.1017	C161	0.0247	C211	0.0054
C12	2.2832	C62	0.3342	C112	0.0987	C162	0.0242	C212	0.0053
C13	1.7238	C63	0.327	C113	0.0959	C163	0.0237	C213	0.0052
C14	1.4164	C64	0.3578	C114	0.0931	C164	0.0232	C214	0.0051
C15	2.6905	C65	0.3521	C115	0.0905	C165	0.0227	C215	0.0050
C16	1.2017	C66	0.3457	C116	0.0879	C166	0.0223	C216	0.0049
C17	1.3620	C67	0.3388	C117	0.0855	C167	0.0218	C217	0.0048
C18	1.1397	C68	0.3311	C118	0.0831	C168	0.0214	C218	0.0047
C19	1.1258	C69	0.3233	C119	0.0808	C169	0.0211	C219	0.0046
C20	1.0862	C70	0.3153	C120	0.0786	C170	0.0207	C220	0.0045
C21	1.0384	C71	0.2948	C121	0.0764	C171	0.0203	C221	0.0044
C22	1.0429	C72	0.2867	C122	0.0743	C172	0.0199	C222	0.0043
C23	0.9724	C73	0.2787	C123	0.0722	C173	0.0195	C223	0.0042
C24	0.9558	C74	0.2708	C124	0.0705	C174	0.0191	C224	0.0041
C25	0.8823	C75	0.2631	C125	0.0685	C175	0.0189	C225	0.0040
C26	0.8428	C76	0.2556	C126	0.0660	C176	0.0184	C226	0.0039
C27	0.8126	C77	0.2483	C127	0.0646	C177	0.0181	C227	0.0038
C28	0.7749	C78	0.2413	C128	0.0627	C178	0.0177	C228	0.0037
C29	0.7539	C79	0.2347	C129	0.0609	C179	0.0174	C229	0.0036
C30	0.7522	C80	0.2285	C130	0.0591	C180	0.0170	C230	0.0035
C31	0.7092	C81	0.2227	C131	0.0573	C181	0.0167	C231	0.0034
C32	0.6729	C82	0.2173	C132	0.0555	C182	0.0164	C232	0.0033
C33	0.6482	C83	0.2123	C133	0.0539	C183	0.0161	C233	0.0032
C34	0.6284	C84	0.2077	C134	0.0522	C184	0.0158	C234	0.0031
C35	0.6143	C85	0.2039	C135	0.0506	C185	0.0155	C235	0.0030
C36	0.5990	C86	0.1992	C136	0.0490	C186	0.0152	C236	0.0029
C37	0.5776	C87	0.1953	C137	0.0475	C187	0.0149	C237	0.0028
C38	0.5559	C88	0.1914	C138	0.0461	C188	0.0146	C238	0.0027
C39	0.5356	C89	0.1877	C139	0.0446	C189	0.0143	C239	0.0026
C40	0.5188	C90	0.1840	C140	0.0433	C190	0.0140	C240	0.0025
C41	0.5060	C91	0.1803	C141	0.0420	C191	0.0137	C241	0.0024
C42	0.4914	C92	0.1765	C142	0.0407	C192	0.0134	C242	0.0023
C43	0.4772	C93	0.1746	C143	0.0395	C193	0.0131	C243	0.0022
C44	0.4641	C94	0.1705	C144	0.0382	C194	0.0128	C244	0.0021
C45	0.5694	C95	0.1664	C145	0.0370	C195	0.0126	C245	0.0020
C46	0.5530	C96	0.1621	C146	0.0360	C196	0.0123	C246	0.0019
C47	0.5370	C97	0.1578	C147	0.0350	C197	0.0120	C247	0.0018
C48	0.5207	C98	0.1535	C148	0.0340	C198	0.0117	C248	0.0017
C49	0.5037	C99	0.1491	C149	0.0330	C199	0.0115	C249	0.0016
C50	0.5080	C100	0.1447	C150	0.0322	C200	0.0084	C250	0.0028

Figure 5-107. Highly Dispersed Ruthenium Catalyst 4966-72 Conversions in Run 18
(H₂:CO Feed Ratio = 2.9, 208°C at Inlet, 35 atm)

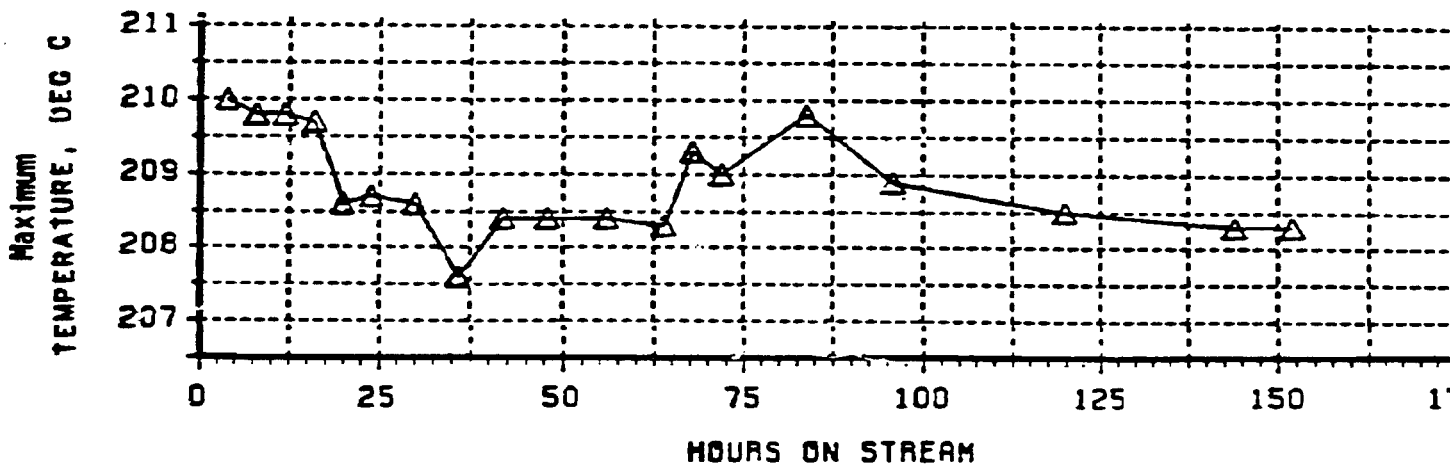
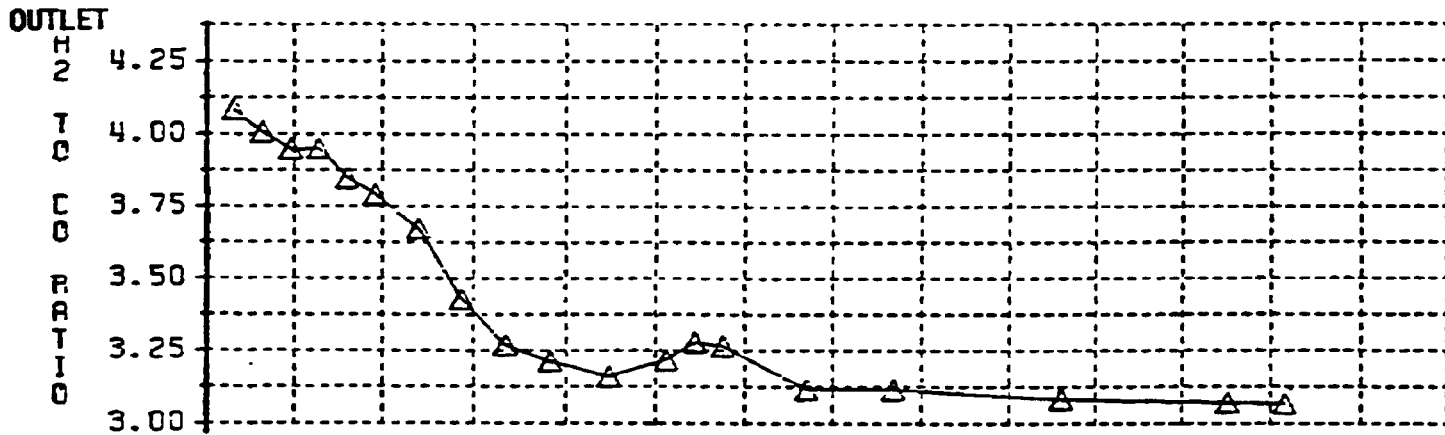
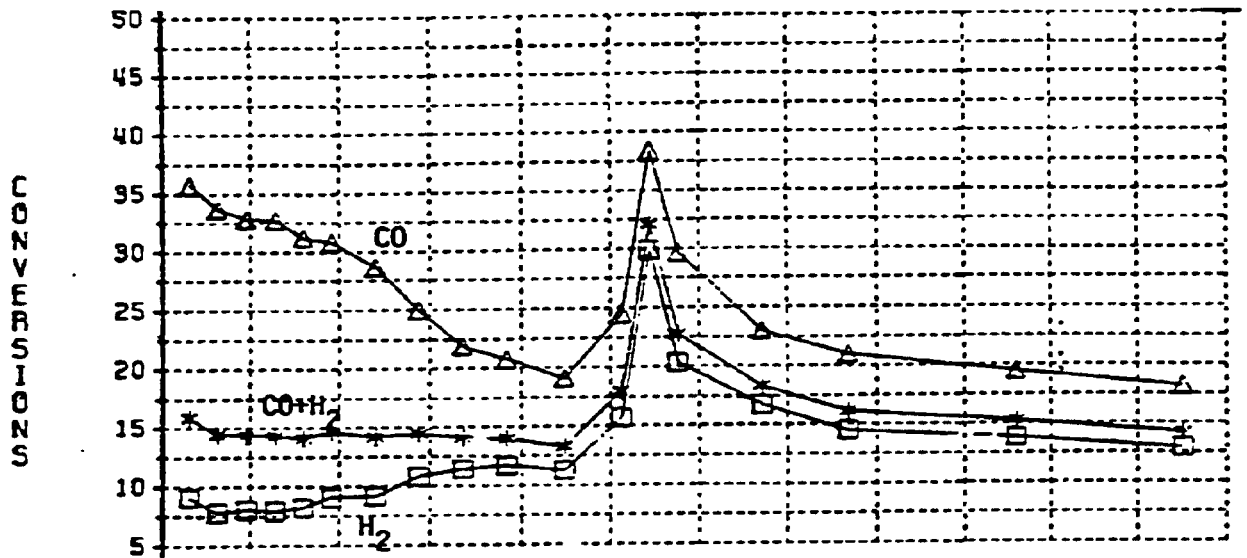


Figure 5-108. Highly Dispersed Ruthenium Catalyst 4966-72 Water Gas Shift Activity in Run 18 ($H_2:CO$ Feed Ratio = 2.9, $208^\circ C$ at Inlet, 35 atm)

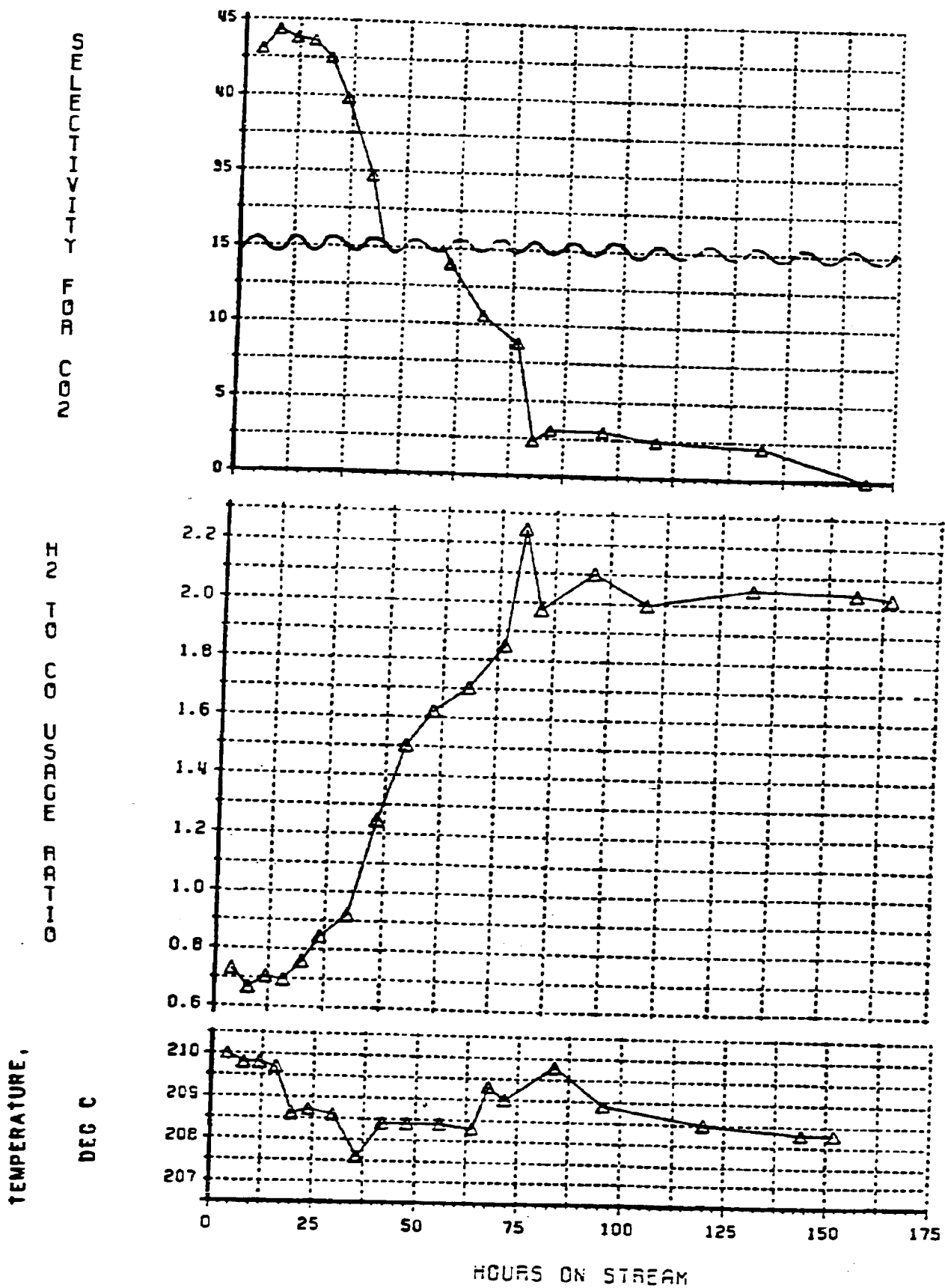


Figure 5-109. Highly Dispersed Ruthenium Catalyst 4966-72 C₁ and C₂ Selectivities in Run 18 (H₂:CO Feed Ratio = 2.9, 208°C at Inlet, 35 atm)

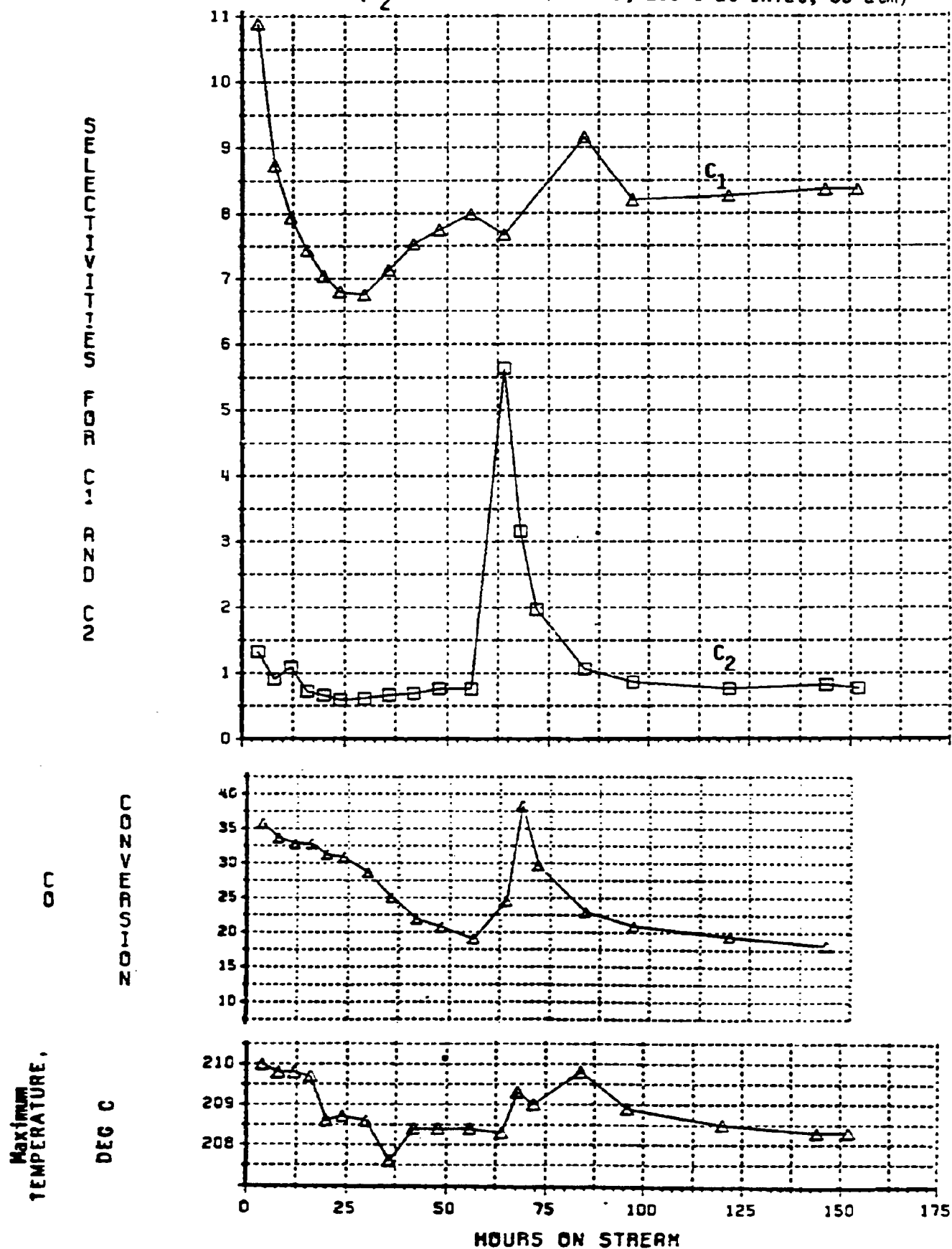


Figure 5-110. Highly Dispersed Ruthenium Catalyst 4966-72 C₃ and C₄ Selectivity in Run 18 (H₂:CO Feed Ratio = 2.9, 208°C at Inlet, 35 atm)

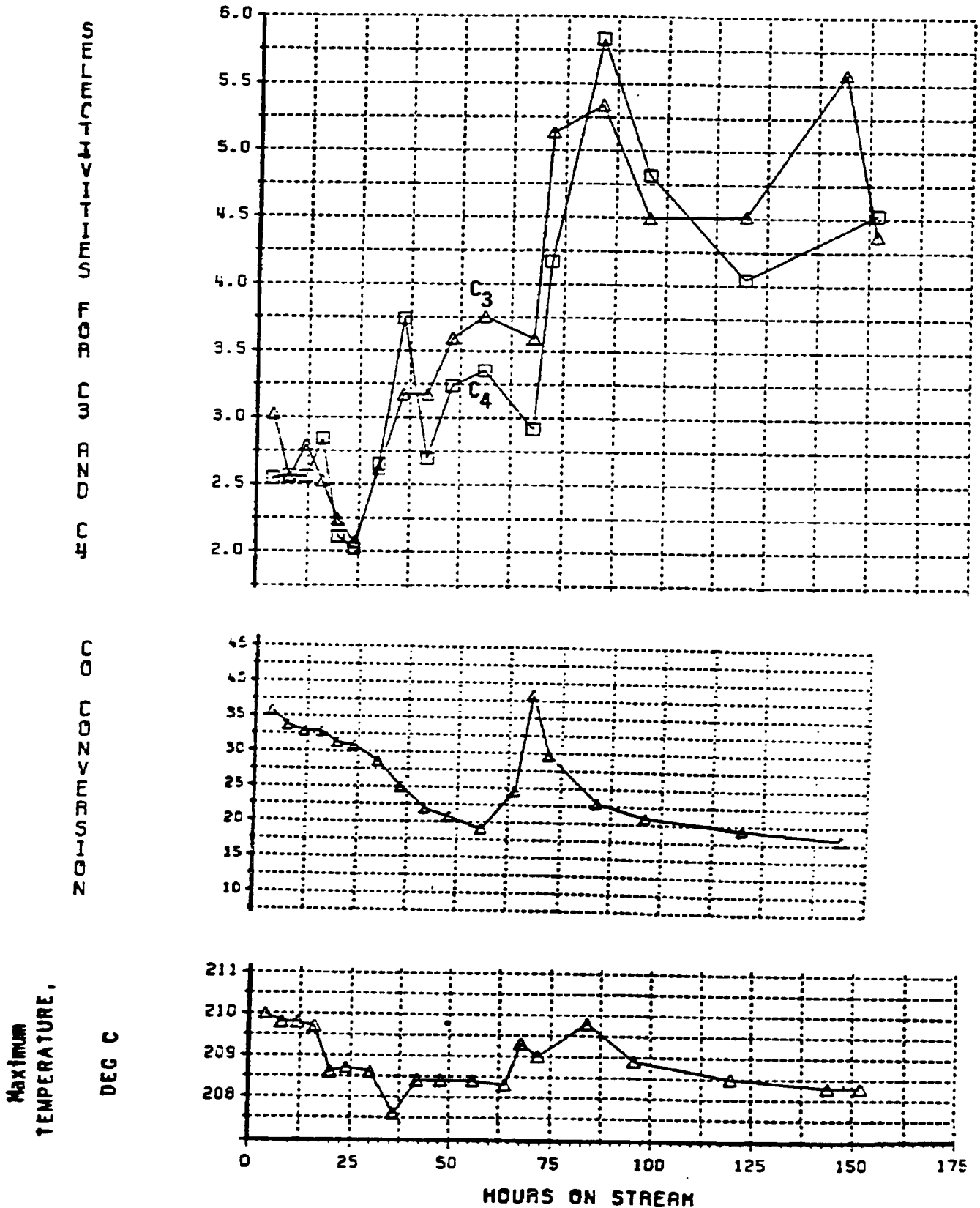


Figure 5-111. Highly Dispersed Ruthenium Catalyst 4966-72 Olefin to Paraffin Ratios in Run 18 ($H_2:CO$ Feed Ratio = 2.9, $208^\circ C$ at Inlet, 35 atm)

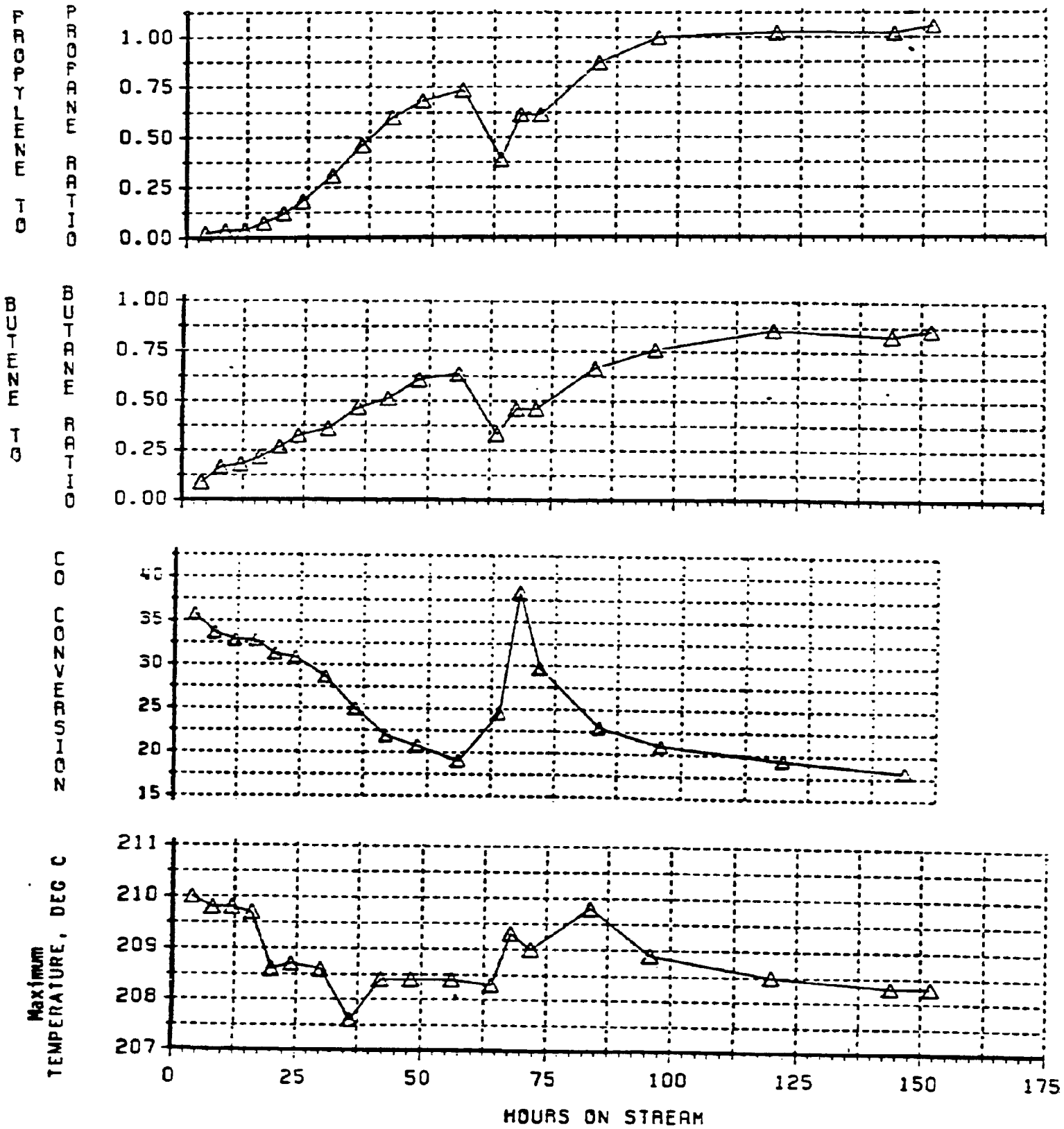


Figure 5-112. Anderson-Schulz-Flory Distribution with Highly Dispersed Ruthenium Catalyst 4966-72 in Run 18 (Hydrocarbons + Oxygenates)

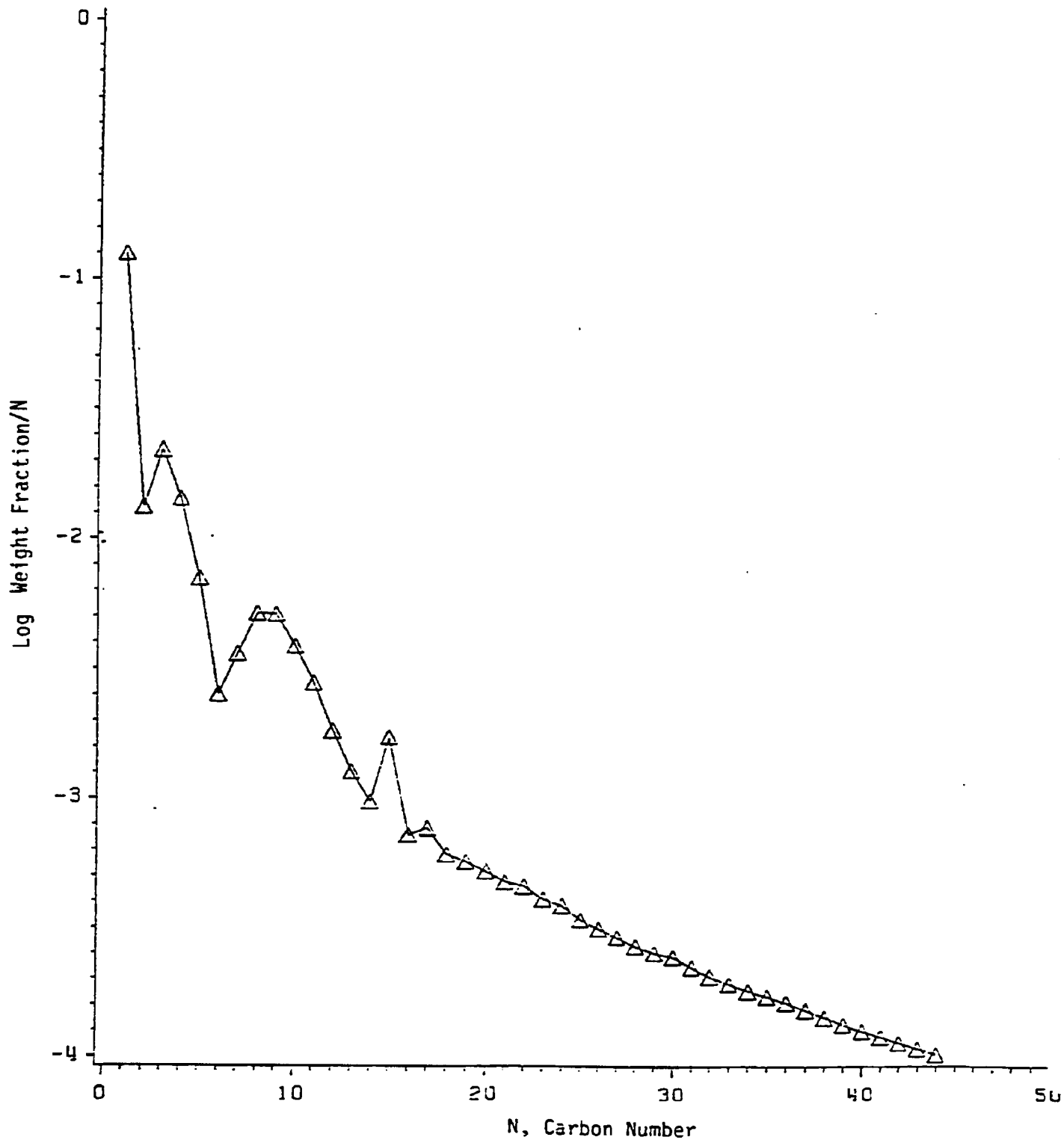
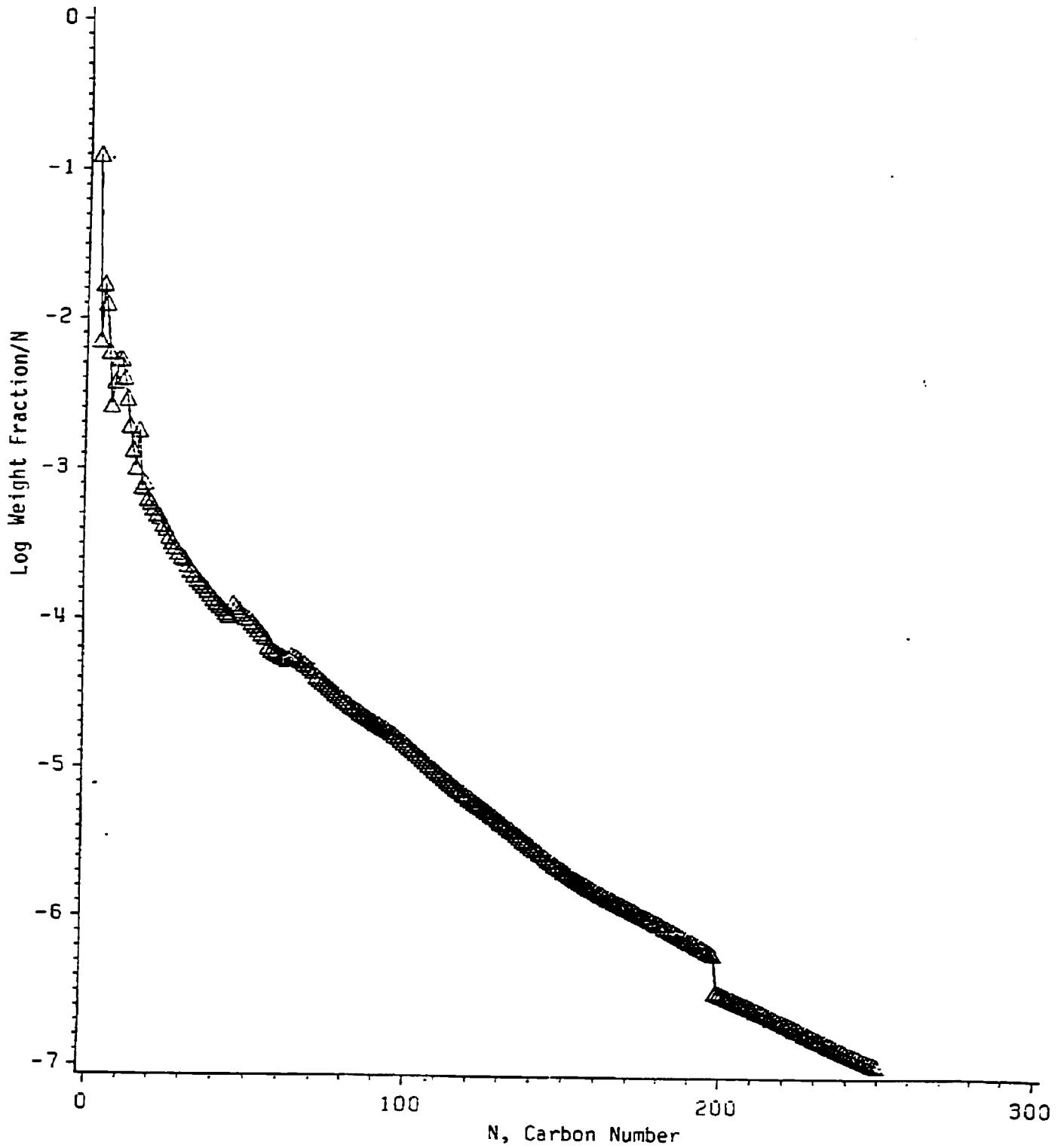


Figure 5-113. Anderson-Schulz-Flory Distribution with Highly Dispersed Ruthenium Catalyst 4966-72 in Run 18 (Hydrocarbons Only)



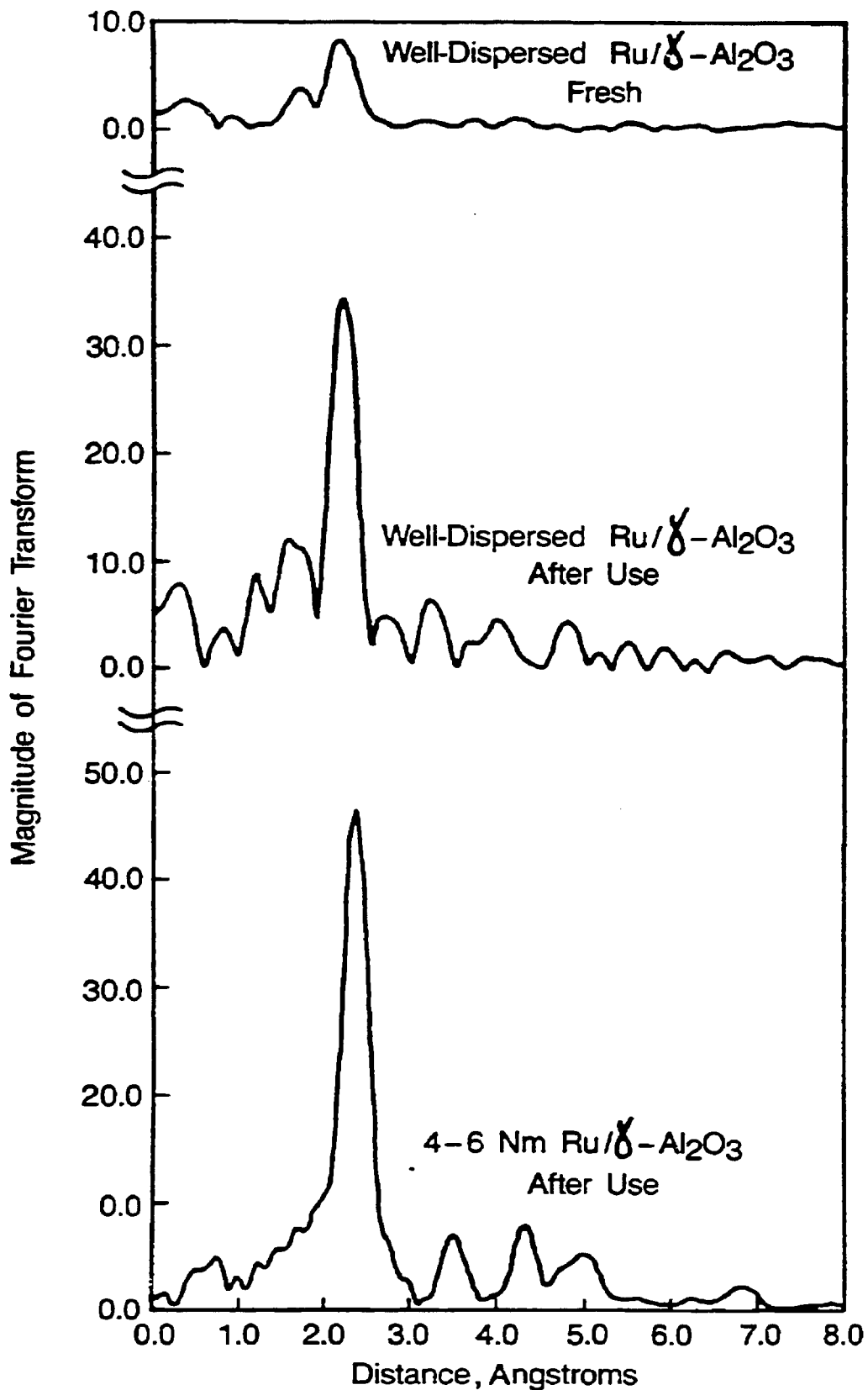
The chain growth probability was 0.783 at C₃-C₁₆, 0.918 at C₁₇-C₃₀ and 0.964 at C₄₀-C₁₅₀ carbon number ranges. Comparison of these results with those obtained in Run 16 with another highly dispersed ruthenium catalyst at a lower H₂:CO feed ratio = 0.9 may indicate that H₂:CO ratio mainly influences the chain growth probabilities at low carbon numbers, but not at high carbon numbers.

Analysis of the inlet and outlet portions of the catalyst after a 152-hour-test showed 0.925% and 1.13% (by wt.) ruthenium, respectively. Although there was no overall ruthenium loss from the catalyst, some ruthenium migration still occurred across the catalyst bed. The mobility of ruthenium was also apparent in the STEM examination. While approximately 60% of the alumina particles examined from the inlet portion of the catalyst bed did not have observable ruthenium particles, 40% of the alumina particles still had 3-15 nm ruthenium particles. The number of alumina particles with observable ruthenium metal particles was half for the outlet portion of the catalyst bed relative to the inlet.

A sample from the reactor inlet portion of used Catalyst 4966-72 was analyzed by EXAFS.

The Fourier transform oscillations of ruthenium in fresh Catalyst 4966-72 is shown in Figure 5-114. The major peak at about 2.2Å results from back-scattering of electrons from nearest neighbors. From a curve-fitting analyses of the Fourier filtered χ , a coordination number of about 3.4 was determined which should give a ruthenium metal particle size of about 0.8 nm. The Fourier transform of the used Catalyst 4966-72 is very similar to that of Catalyst 4956-76 with 4-6 nm ruthenium particles after use in Run 15. This result confirms the STEM observation that a significant fraction of the ruthenium metal agglomerated to sizes 4 nm or larger during Fischer-Tropsch synthesis.

Figure 5-114 **FOURIER TRANSFORMS OF RUTHENIUM EXAFS
IN ALUMINA SUPPORTED CATALYSTS**



The results in Run 18 indicated that mobility of ruthenium was suppressed but not totally eliminated, apparently, by increasing the $H_2:CO$ feed ratio from 0.9 to 2.9. At the higher $H_2:CO$ ratio, the mobility of ruthenium may have been suppressed by suppressing the formation of the volatile ruthenium carbonyl.

Highly dispersed ruthenium Catalyst 4966-72 was retested in Run 21 under the same conditions that were used in Run 18, but only for 12 hours (Tables 5-22 and 5-23 and Figures 5-115 through 5-121). The $CO+H_2$ conversion was much higher in Run 21 relative to Run 18 (Figure 5-115). The unexpectedly lower catalytic activity in Run 18 may be possibly attributed to the unusually long start-up for that run.

The CO conversion was 100% during the second half of Run 21 (Figure 5-115). Since the H_2 conversion was less than 100% the outlet $H_2:CO$ ratio became infinitely large. This caused very high selectivity to methane and apparently caused the extent of the water gas shift reaction to become minimal (Figure 5-116).

Because of the short duration of the test, products in the C_5-C_{23} range were not fully recovered in the product receivers. The chain growth probability was 0.936 in the $C_{24}-C_{150}$ range.

The inlet and outlet portions of Catalyst 4966-72 used in Run 21 showed less ruthenium than fresh catalyst: 0.81% and 0.84% Ru (by wt.), respectively, relative to 1.04% Ru on the fresh catalyst. STEM examination indicated that almost all of the alumina particles had 2-5 nm agglomerated ruthenium particles, while the fresh catalyst had none. The possibility that the high steam partial pressure, caused by suppression of the water gas shift reaction in Run 21, may have enhanced ruthenium agglomeration was further investigated in Run 25.

Table 5-22. Product D, Contributions in Run 21

GAS ANALYSIS, WT%			
HYDROGEN	5.5624	HEIGHT PCTS WITHOUT ARGON	5.562
CARBON MONOXIDE	4.8440	HYDROGEN	4.844
CARBON DIOXIDE	9.9460	CARBON MONOXIDE	9.946
METHANE	8.4129	CARBON DIOXIDE	48.615
ETHANE	0.4604	WATER	30.022
ETHYLENE	0.0000	HYDROCARBONS	0.210
PROPANE	1.2307	OXYGENATES	
PROPYLENE	0.0000		
BUTANE	1.4738		
BUTENE	0.0000		
AQUEOUS ANALYSIS, WT%			
WATER	48.6152	HYDROCARBON DISTRIBUTION	
ALCOHOLS		C1	27.295
C1	0.0000	C2 - C4	10.268
C2	0.0463	C5 - C11	16.220
C3	0.0000	C12 - C18	4.516
C4	0.0472	C19 - C25	5.165
C5	0.0702	C26 PLUS	36.536
C6	0.0463	C1 - C44	79.392
C7	0.0000	C45 PLUS	20.608
C8	0.0000		
C9	0.0000		
C10	0.0000		
ALDEHYDES		OXYGENATES DISTRIBUTION	
C1	0.0000	ALCOHOLS	100.000
C2	0.0000	ALDEHYDES	0.000
C3	0.0000	OTHER OXYGENATES	0.000
C4	0.0000		
C5	0.0000		
C6	0.0000		
C7	0.0000		
C8	0.0000		
C9	0.0000		
C10	0.0000		
OTHER OXYGENATES		HOLE PCTS WITHOUT ARGON	
C1	0.0000	HYDROGEN	42.254
C2	0.0000	CARBON MONOXIDE	2.648
C3	0.0000	CARBON DIOXIDE	3.461
C4	0.0000	WATER	41.527
C5	0.0000	HYDROCARBONS	10.265
C6	0.0000	OXYGENATES	0.044
C7	0.0000		
C8	0.0000		
C9	0.0000		
C10	0.0000		
RECOVERIES		OVERALL	75.143
C1	0.0000	CARBON	65.510
C2	0.0000	HYDROGEN	73.986
C3	0.0000	OXYGEN	86.776
C4	0.0000	ARGON	67.957
C5	0.0000		
C6	0.0000		
C7	0.0000		
C8	0.0000		
C9	0.0000		
C10	0.0000		
CORRECTED RECOVERIES		OVERALL	110.575
C1	0.0000	CARBON	96.400
C2	0.0000	HYDROGEN	108.873
C3	0.0000	OXYGEN	127.693
C4	0.0000		
C5	0.0000		
C6	0.0000		
C7	0.0000		
C8	0.0000		
C9	0.0000		
C10	0.0000		

Table 5-23. Hydrocarbon Distributions in Run 21

C1	27.2948	0.6101	C101	0.0777	C151	0.0000	C201	0.0000
C2	1.4937	0.5919	C102	0.0742	C152	0.0000	C202	0.0000
C3	3.9928	0.5742	C103	0.0708	C153	0.0000	C203	0.0000
C4	4.7815	0.5571	C104	0.0677	C154	0.0000	C204	0.0000
C5	3.1974	0.5405	C105	0.0647	C155	0.0000	C205	0.0000
C6	2.0162	0.5245	C106	0.0624	C156	0.0000	C206	0.0000
C7	1.5906	0.5072	C107	0.0598	C157	0.0000	C207	0.0000
C8	1.9019	0.4923	C108	0.0573	C158	0.0000	C208	0.0000
C9	2.6048	0.4777	C109	0.0549	C159	0.0000	C209	0.0000
C10	2.6960	0.4636	C110	0.0527	C160	0.0000	C210	0.0000
C11	2.2133	0.4498	C111	0.0506	C161	0.0000	C211	0.0000
C12	1.6523	0.4376	C112	0.0486	C162	0.0000	C212	0.0000
C13	1.0674	0.4243	C113	0.0467	C163	0.0000	C213	0.0000
C14	0.5881	0.4112	C114	0.0449	C164	0.0000	C214	0.0000
C15	0.3301	0.3984	C115	0.0432	C165	0.0000	C215	0.0000
C16	0.1918	0.3858	C116	0.0416	C166	0.0000	C216	0.0000
C17	0.4002	0.3734	C117	0.0400	C167	0.0000	C217	0.0000
C18	0.2858	0.3613	C118	0.0384	C168	0.0000	C218	0.0000
C19	0.3082	0.3484	C119	0.0370	C169	0.0000	C219	0.0000
C20	0.3402	0.3368	C120	0.0356	C170	0.0000	C220	0.0000
C21	0.5335	0.3254	C121	0.0343	C171	0.0000	C221	0.0000
C22	0.8130	0.3141	C122	0.0330	C172	0.0000	C222	0.0000
C23	0.9549	0.3031	C123	0.0318	C173	0.0000	C223	0.0000
C24	1.1143	0.2921	C124	0.0306	C174	0.0000	C224	0.0000
C25	1.1013	0.2812	C125	0.0295	C175	0.0000	C225	0.0000
C26	1.0967	0.2713	C126	0.0284	C176	0.0000	C226	0.0000
C27	1.0745	0.2606	C127	0.0274	C177	0.0000	C227	0.0000
C28	1.0500	0.2499	C128	0.0264	C178	0.0000	C228	0.0000
C29	0.9977	0.2393	C129	0.0255	C179	0.0000	C229	0.0000
C30	0.9986	0.2289	C130	0.0246	C180	0.0000	C230	0.0000
C31	0.9522	0.2186	C131	0.0237	C181	0.0000	C231	0.0000
C32	0.9079	0.2085	C132	0.0229	C182	0.0000	C232	0.0000
C33	0.8747	0.1987	C133	0.0220	C183	0.0000	C233	0.0000
C34	0.8434	0.1892	C134	0.0212	C184	0.0000	C234	0.0000
C35	0.8189	0.1791	C135	0.0205	C185	0.0000	C235	0.0000
C36	0.7923	0.1701	C136	0.0188	C186	0.0000	C236	0.0000
C37	0.7613	0.1615	C137	0.0191	C187	0.0000	C237	0.0000
C38	0.7325	0.1532	C138	0.0185	C188	0.0000	C238	0.0000
C39	0.6878	0.1452	C139	0.0178	C189	0.0000	C239	0.0000
C40	0.6722	0.1378	C140	0.0172	C190	0.0000	C240	0.0000
C41	0.6585	0.1304	C141	0.0166	C191	0.0000	C241	0.0000
C42	0.6408	0.1235	C142	0.0161	C192	0.0000	C242	0.0000
C43	0.6275	0.1170	C143	0.0155	C193	0.0000	C243	0.0000
C44	0.6208	0.1108	C144	0.0150	C194	0.0000	C244	0.0000
C45	0.7308	0.1050	C145	0.0144	C195	0.0000	C245	0.0000
C46	0.7079	0.0997	C146	0.0139	C196	0.0000	C246	0.0000
C47	0.6888	0.0947	C147	0.0134	C197	0.0000	C247	0.0000
C48	0.6678	0.0900	C148	0.0129	C198	0.0000	C248	0.0000
C49	0.6477	0.0856	C149	0.0124	C199	0.0000	C249	0.0000
C50	0.6282	0.0815	C150	0.0119	C200	0.0000	C250	0.0000

Figure 5-115. Highly Dispersed Ruthenium Catalyst 4966-72 Conversions in Run 21 (H₂:CO Feed Ratio = 2.9, 208°C at Inlet, 35 atm)

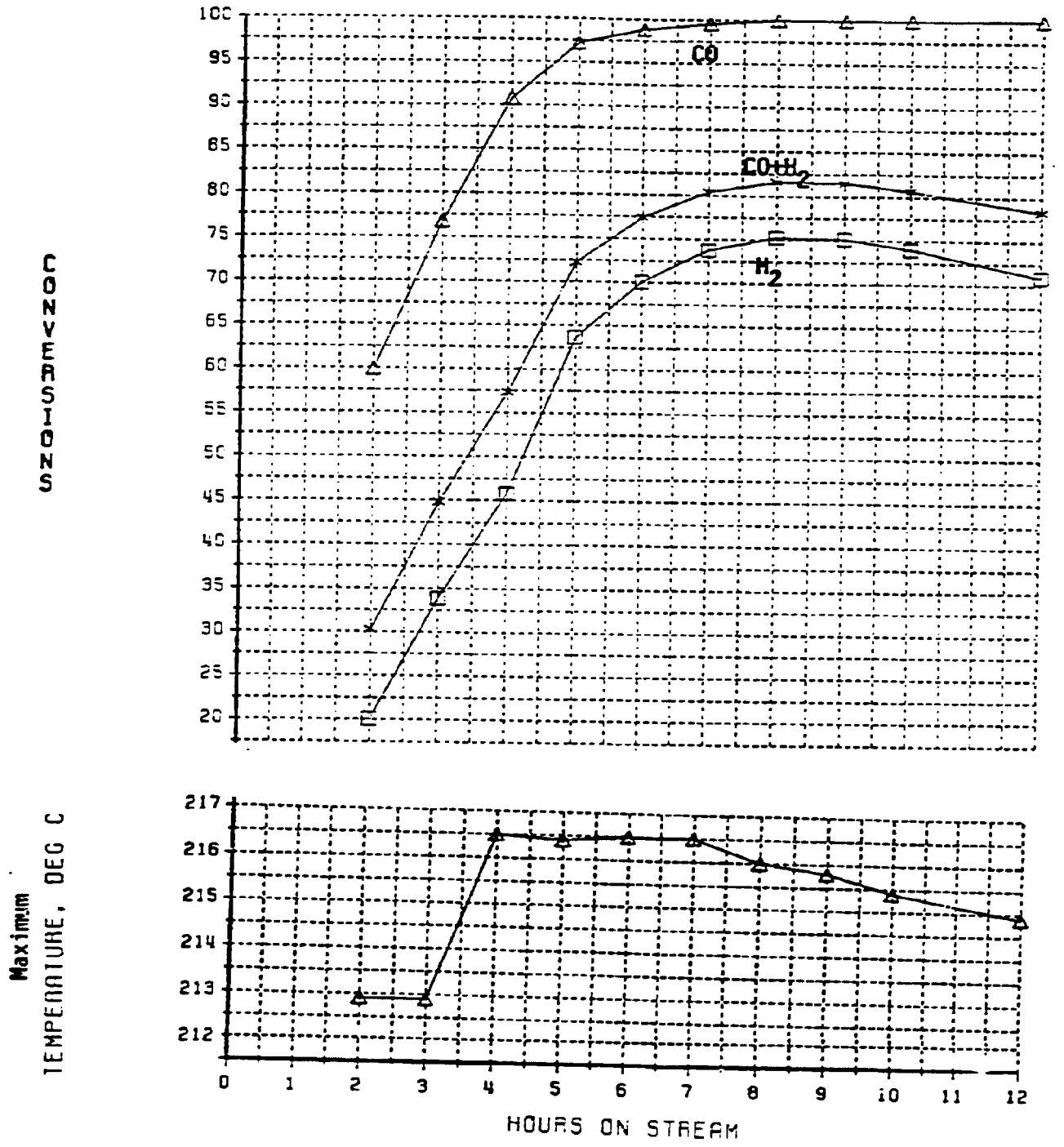


Figure 5-116. Highly Dispersed Ruthenium Catalyst 4966-72 Water Gas Shift Activity in Run 21 ($H_2:CO$ Feed Ratio = 2.9, $208^\circ C$ at Inlet, 35 atm)

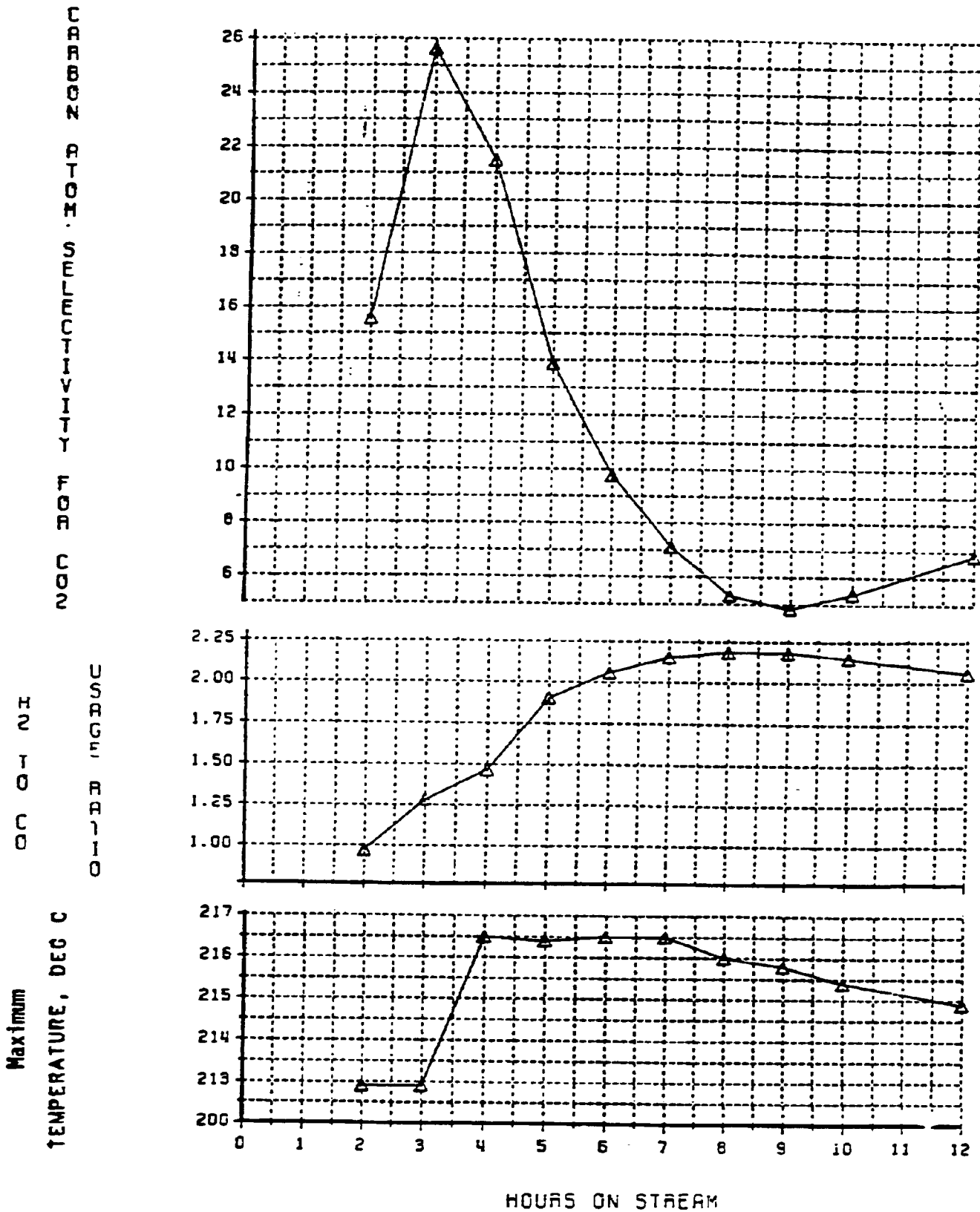


Figure 5-117. Highly Dispersed Ruthenium Catalyst 4966-72 C₁ and C₂ Selectivities in Run 21 (H₂:CO Feed Ratio = 2:9, 208°C, 35 atm)

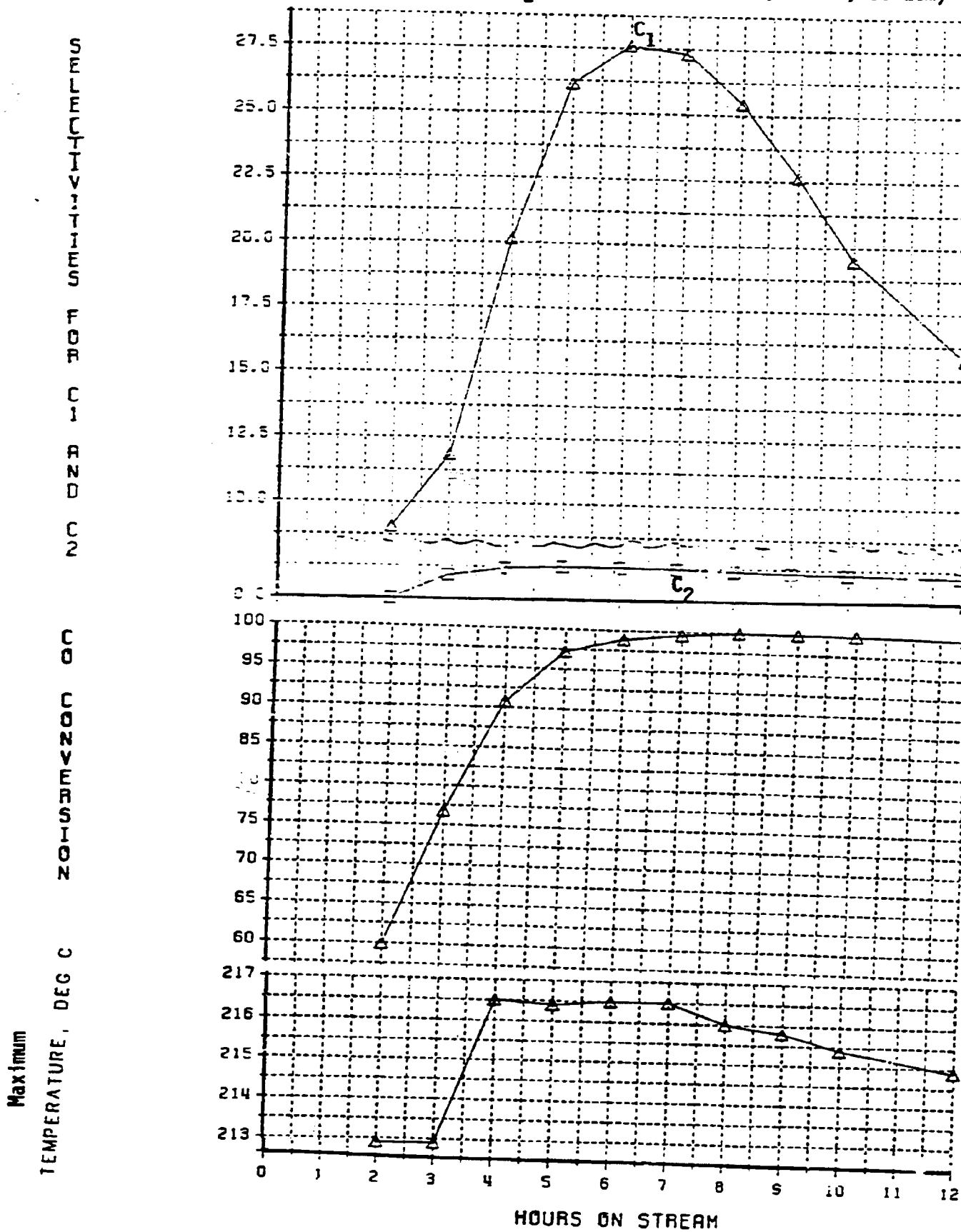


Figure 5-118. Highly Dispersed Ruthenium Catalyst 4966-72 C₃ and C₄ Selectivities in Run 21 (H₂:CO Feed Ratio = 2.9, 208°C at Inlet, 35 atm)

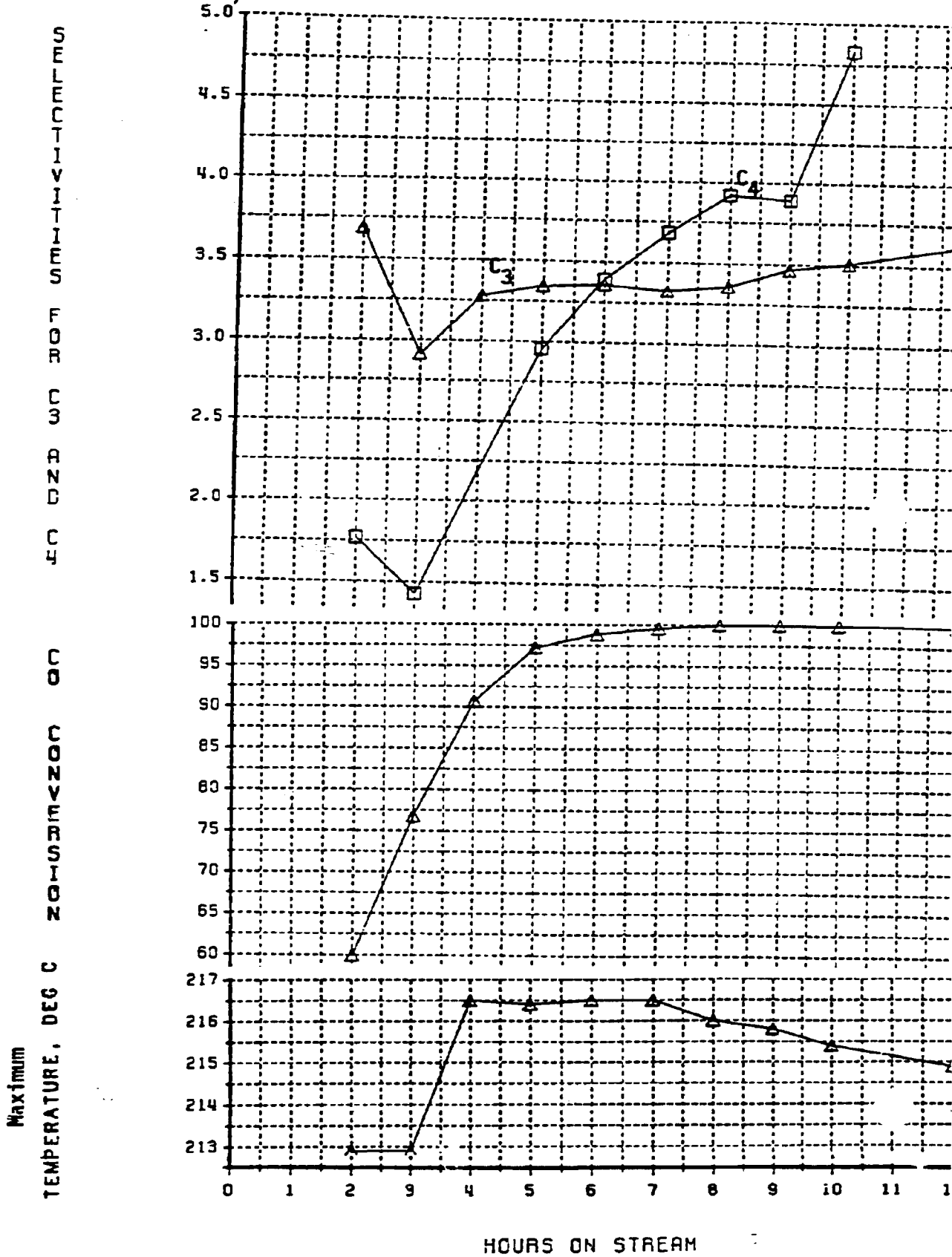


Figure 5-119. Highly Dispersed Ruthenium Catalyst 4966-72 Olefin to Paraffin Ratios in Run 21 ($H_2:CO$ Feed Ratio = 2.9, 208°C at Inlet, 35 atm)

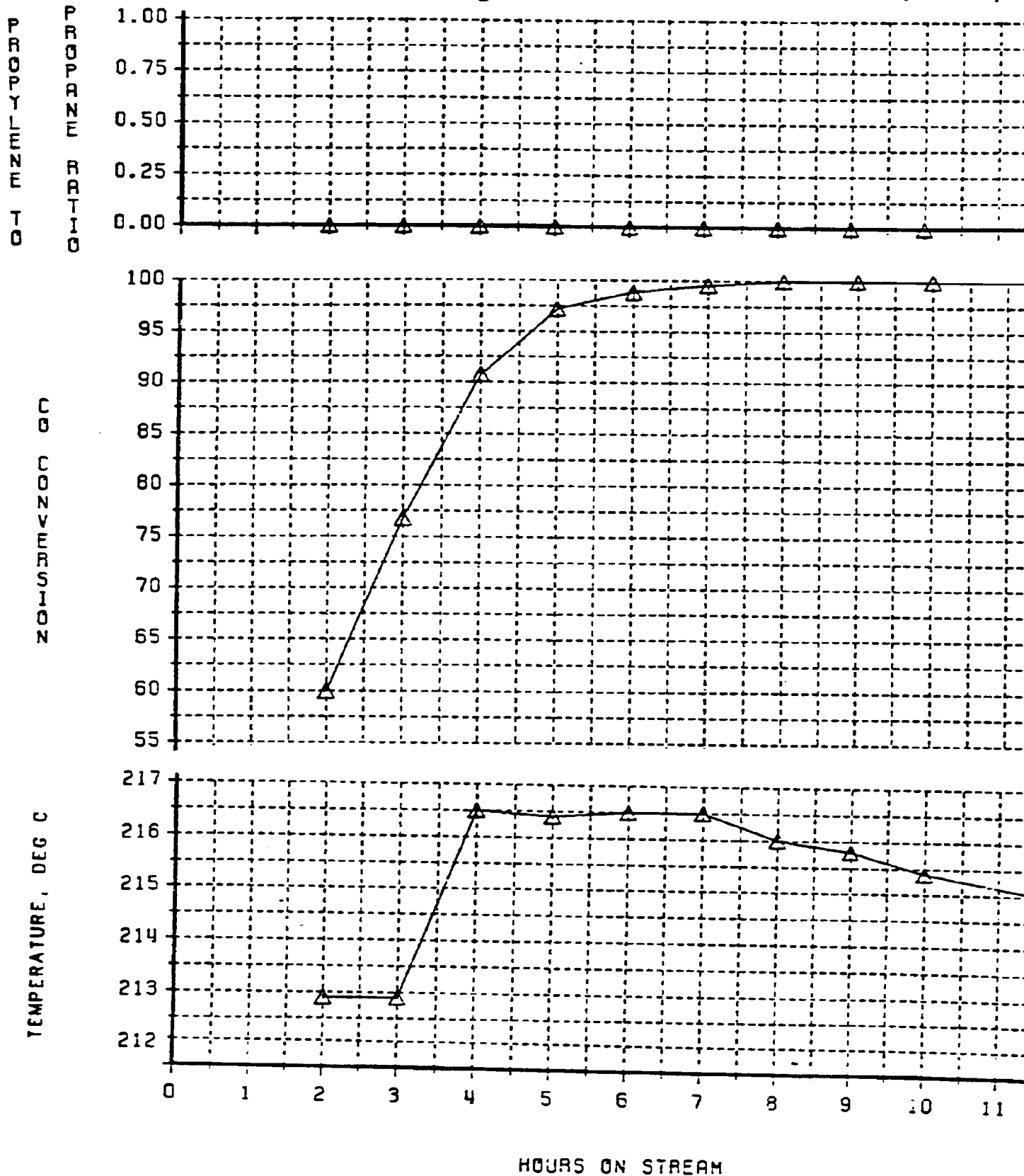


Figure 5-120. Anderson-Schulz-Flory Distribution with Highly Dispersed Ruthenium Catalyst 4966-72 in Run 21 (Hydrocarbons + Oxygenates; C_1-C_{44})

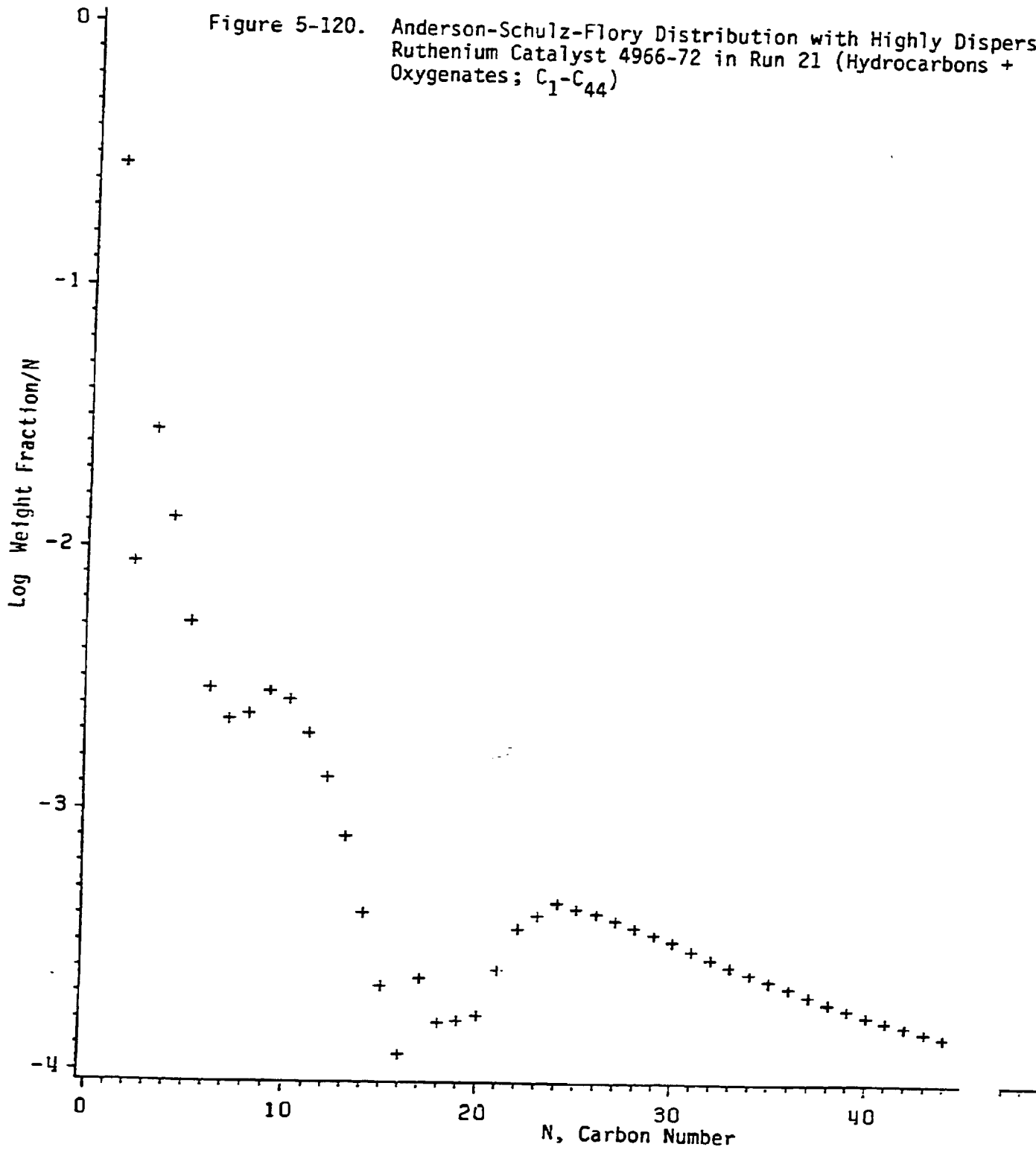


Figure 5-121. Anderson-Schulz-Flory Distribution with Highly Dispersed Ruthenium Catalyst 4966-72 in Run 21 (Hydrocarbons Only; C_1-C_{250})

